IL-6-Driven Autocrine Lactate Promotes Immune Escape of Uveal Melanoma

Chaoju Gong,[1] Meiling Yang,[1] Huirong Long,[1,2] Xia Liu,[3] Qing Xu,[1] Lei Qiao,[1] Haibei Dong,[4] Yalu Liu,[2] and Suyan Li[1,2]

[1]Xuzhou Key Laboratory of Ophthalmology, The Affiliated Xuzhou Municipal Hospital of Xuzhou Medical University, Xuzhou First People's Hospital, Eye Institute of Xuzhou, Xuzhou, China
[2]Department of Ophthalmology, The Affiliated Xuzhou Municipal Hospital of Xuzhou Medical University, Xuzhou First People's Hospital, Eye Institute of Xuzhou, Xuzhou, China
[3]Department of Pathology, The Affiliated Xuzhou Municipal Hospital of Xuzhou Medical University, Xuzhou First People's Hospital, Xuzhou, China
[4]Cancer Center, The Affiliated Xuzhou Municipal Hospital of Xuzhou Medical University, Xuzhou First People's Hospital, Xuzhou, China

PURPOSE. Early metastasis, in which immune escape plays a crucial role, is the leading cause of death in patients with uveal melanoma (UM); however, the molecular mechanism underlying UM immune escape remains unclear, which greatly limits the clinical application of immunotherapy for metastatic UM.

METHODS. Transcriptome profiles were revealed by RNA-seq analysis. TALL-104 and NK-92MI-mediated cell killing assays were used to examine the immune resistance of UM cells. The glycolysis rate was measured by extracellular acidification analysis. Protein stability was evaluated by CHX-chase assay. Immunofluorescence histochemistry was performed to detect protein levels in clinical UM specimens.

RESULTS. Continuous exposure to IL-6 induced the expression of both PD-L1 and HLA-E in UM cells, which promoted UM immune escape. Transcriptome analysis revealed that the expression of most metabolic enzymes in the glycolysis pathway, especially the rate-limiting enzymes, PFKP and PKM, was upregulated, whereas enzymes involved in the acetyl-CoA synthesis pathway were downregulated after exposure to IL-6. Blocking the glycolytic pathway and lactate production by knocking down PKM and LDHA decreased PD-L1 and HLA-E protein, but not mRNA, levels in UM cells treated with IL-6. Notably, lactate secreted by IL-6-treated UM cells was crucial in influencing PD-L1 and HLA-E stability via the GPR81-cAMP-PKA signaling pathway.

CONCLUSIONS. Our data reveal a novel mechanism by which UM cells acquire an immune-escape phenotype by metabolic reprogramming and reinforce the importance of the link between inflammation and immune escape.

Keywords: uveal melanoma (UM), immune escape, interleukin-6, glycolysis, lactate

Uveal melanoma (UM) is the most common intraocular malignancy in adults. Although very few patients present with detectable metastases at diagnosis of primary UM, up to half of patients with UM eventually develop metastases.[1] A mathematical modeling for UM metastasis suggests that micro-metastases will begin before the primary tumor is diagnosed.[2] Metastatic UM has a poor prognosis, with an average overall survival (OS) of less than 1 year.[3] Although primary UM can be effectively controlled by enucleation and plaque radiotherapy, the therapeutic effects of conventional chemotherapy on metastatic UM remain unsatisfactory.[4] In recent years, immunotherapy has shown promise for the treatment of various malignant tumors, including metastatic cutaneous melanoma[5]; however, immunotherapy targeting UM currently remains at an exploratory stage.[6,7] At present, the molecular mechanism underlying immune escape during UM metastasis is unclear, which greatly limits the clinical

application of immunotherapy in metastatic UM. Therefore, elucidation of the key mechanisms underlying UM immune escape is of great scientific significance and clinical value, and will help in identification of markers and therapeutic targets for early UM metastasis.

Immune escape plays an important role in the development of malignant tumors, during which tumor cells alter immune regulatory factors and the microenvironment directly, to avoid recognition and clearance by immune cells. The eyeball is an immune-privileged organ that provides a protective growth environment for UM. Further, there is evidence that UM cells can also maintain immune escape, and resistance to cell-mediated immunity has an important role during metastasis.[1,8] Programmed death ligand 1 (PD-L1) is expressed on the surface of tumor cells and binds to the PD-1 receptor on activated T cells, leading to suppression of T lymphocyte proliferation, cytokine

Investigative Ophthalmology & Visual Science

production, and immune responses.[9] In vitro studies have shown that the local microenvironment can induce UM cells to overexpress PD-L1, thereby negatively regulating T cell-mediated immune responses.[10] Furthermore, PD-L1 is negatively correlated with OS, progression-free survival, and tumor thickness in patients with UM[11]; however, compared with cutaneous melanoma, the clinical efficacy of PD-1/PD-L1 antibody-based drugs for the treatment of metastatic UM requires further improvement.[12,13] Human leukocyte antigen (HLA) levels are upregulated in UM cells, facilitating their escape from the killing effects of cytotoxic T and natural killer (NK) cells in the tumor microenvironment (TME).[14] In addition, elevated HLA expression is associated with shorter metastasis-free survival in patients with UM,[15] in which HLA-E binds to NKG2A expressed by subsets of NK and CD8$^+$ T cells and negatively regulates their antitumor immune activity.[16] Notably, melanoma can express high levels of HLA-E to prevent NK cell recognition.[17] During metastasis, circulating tumor cells can evade immune surveillance by circulating T and NK cells through activation of the above inhibitory immune checkpoints PD-L1 and HLA-E. Hence, multiple immunosuppressive molecules may be involved in the immune escape of metastatic UM; however, it remains unclear how the TME induces UM cells to express diverse immunosuppressive molecules during metastasis.

As an important part of the TME, inflammation has a key role in promoting tumor metastasis, in which various inflammatory factors secreted by mesenchymal cells, such as inflammatory immune cells and autocrine tumor cells, promote malignant transformation. Chronic, low-intensity inflammatory responses promote tumor invasion, early metastasis, and immune escape.[18] In UM, an inflammatory phenotype, with infiltration of different lymphocytes and macrophages, is associated with absence of effective antitumor immune responses.[19] Early studies found that the levels of several inflammatory factors, including IL-6, IL-8, IP-10, MCP-1, and RANTES, were abnormally elevated in the intraocular fluid of patients with UM.[20] In addition, the expression of IL-6 in hepatic stellate cells increases significantly after co-culture with metastatic UM cells, which may be associated with the process of UM liver metastasis.[21] Clinical analysis has shown that activation of IL-6/STAT3 signaling is closely related to poor prognosis of patients with UM[22]; however, until now, most studies have focused solely on the concentrations of different inflammatory factors in the eyes of patients with UM, whereas the roles of these factors in UM progression have rarely been reported.

In this study, we demonstrated immune escape of UM mediated by the inflammatory cytokine, IL-6. Continuous exposure to IL-6 activated the glycolytic metabolic pathway of UM cells, thus promoting the production of lactate. Further, we found that UM cell-derived lactate binds to the lactate receptor, GPR81, thereby reducing intracellular cAMP levels, and inhibiting the ubiquitination and degradation of PD-L1 and HLA-E, and finally enhancing UM resistance to cytotoxic T and NK cell-mediated killing.

MATERIALS AND METHODS

Cell Culture and Transfection

C918, a human UM cell line established from choroidal melanomas with epithelioid type morphology, was purchased from the National Infrastructure of Cell Line Resource (Beijing, China) and cultured in RPMI-1640 medium containing 10% fetal bovine serum (Gibco, Waltham, MA, USA), 100 U/mL penicillin, and 100 mg/mL streptomycin. Mycoplasma was tested by PCR every 3 months. IL-6-exposed C918 cells (IL-6/C918) were obtained by treatment with 2 ng/mL IL-6 (#200-06; PeproTech, USA, Endotoxin < 1 EU/µg) for 8 weeks, and were subsequently maintained in medium supplemented with 2 ng/mL IL-6. Cells were cultured in a 5% CO_2 atmosphere at 37°C. SiRNAs were transfected using Lipofectamine 3000 Transfection Reagent (Life Technologies, Carlsbad, CA, USA), according to the manufacturer's instructions. Briefly, opti-MEM was used to dilute siRNA (75 pmol/well/6-well plate) and Lipofectamine 3000 (7.5 µL/well/6-well plate), and the 2 diluents then mixed (1:1) to prepare an siRNA-liposome complex, which was added into culture medium. Cells were cultured for 48 hours before experiments.

RNA-Seq Analysis

RNA from IL-6/C918 or C918 cells was extracted and purified for quantification, RNA-seq library preparation, and sequencing. Libraries were sequenced on the Illumina HiSeq 2500 platform. Reads containing adapter or poly-N and reads of low quality were removed from the raw data to generate clean reads for further analyses. Q20 (>90%), Q30 (>85%), and error rate (<0.1%) values of clean data were acquired based on clean reads. Mapped reads were then obtained using Tophat2 to align clean reads to the human reference genome (hg19). The number of mapped clean reads for each unigene was counted and normalized to reads/kb/million reads (RPKM), to calculate the expression levels of unigenes.

Antibodies and Reagents

Antibodies against PFKP (sc-514824), PKM (sc-365684), LDHA (sc-137243), PD-L1 (sc-293425), HLA-E (sc-51621), and ubiquitin (sc-8017) were purchased from Santa Cruz Biotechnology (SantaCruz, CA, USA). The IgG isotypes (#3900) were purchased from Cell Signaling Technology (Beverly, MA, USA). GPR81 antibody (A20321) was purchased from Abclonal (Wuhan, China). PD-L1 (ab213524) and HLA-E (ab300553) antibodies were purchased from Abcam (Cambridge, UK). β-actin antibody (E021020-01) was purchased from Earthox (Burlingame, CA, USA). The siRNAs targeting GPR81, PKM, and LDHA were synthesized by GenePharma (Shanghai, China). CHX (M4879) was purchased from Abmole (Houston, TX, USA). Recombinant human IL-6 (200-06) was purchased from Peprotech (Cranbury, NJ, USA). MG-132 (S2619), Sodium oxamate (S6871), Bucladesine (S7858), and forskolin (S2449) were purchased from Selleck (Houston, TX, USA).

Quantitative PCR

Total RNA was isolated with RNAiso Plus (TaKaRa, Kyoto, Japan). RNA quality and concentration were evaluated using a Nanodrop ND-1000 Spectrophotometer. A total of 0.5 µg of RNA was reverse transcribed using a cDNA Reverse Transcription Kit (TaKaRa), according to the manufacturer's instructions. The acquired cDNA was analyzed in triplicate by real-time PCR on a Life Technologies Step One Plus Real-Time PCR System with SYBR Green Master Mix (Roche, Basel, Switzerland). Target gene expression was normalized to β-actin levels in respective samples as an internal control. Relative expression levels were calculated using the $2^{-\Delta\Delta CT}$

method. The sequences of the quantitative real-time PCR (qRT-PCR) primers are listed in Supplementary Table S1.

Western Blotting

Cells were harvested and lysed using RIPA lysis buffer (Millipore, Temecula, CA, USA). After cell lysates were diluted (1:20), protein concentrations were determined using the Bradford method (Pierce, ThermoFisher, Waltham, MA, USA). Proteins were separated by 10% SDS-PAGE and transferred to nitrocellulose membrane (Whatman, Maidstone, UK), which was then incubated with dilutions (1:1000) of primary antibodies, followed by IRDye 800CW-conjugated secondary antibodies (1:10000). Detection was conducted using an Odyssey Infrared Imaging System (LI-COR; Biosciences, Lincoln, NE, USA).

Flow Cytometric Analysis

Cells were digested, collected, and fixed using 2% PFA. Then, cells were washed and labeled with IgG isotype (#3900, 1:2000), PD-L1 (ab213524, 1:500), and HLA-E (ab300553, 1:100) antibodies. Cells were incubated with the indicated primary antibody at room temperature for 30 minutes, then washed and incubated with Alexa Fluor 488-conjugated anti-rabbit IgG (#4412; Cell Signaling Technology, 1:500) in a dark at room temperature for 30 minutes before analysis by flow cytometry. Levels of membrane PD-L1 and HLA-E were measured using an EXFLOW flow cytometer (DAKEWE, Shenzhen, China). Data were analyzed using EXFLOWSYS 1.2.5 (DAKEWE, Shenzhen, China).

TALL-104 and NK-92MI-Mediated Cells Killing Assay

C918 and IL-6/C918 cells were seeded into 6-well plates at a density of 1×10^5 cells per well, and then TALL-104 and NK-92MI cells pretreated with 100 IU/mL IL-2 were introduced into each well, and co-cultured with C918 and IL-6/C918 cells at effector/target cell ratio of 5:1 for 24 hours.[16,23] After co-culture, wells were extensively washed to eliminate dead cells and effector cells, then the adherent C918 and IL-6/C918 cells were harvested and analyzed by using the Annexin V/PI staining kit (Beyotime, Shanghai, China). When specified, IL-6/C918 and C918 cells were pretreated with sodium oxamate and lactate, respectively.

PI-Annexin V Apoptosis Assay

Cells cultured in medium and digested with trypsin were collected. The Annexin V/PI staining kit (Beyotime, Shanghai, China) was utilized to label cells according to the manufacturer's protocol. After filtering through 50 μm mesh, cells were analyzed with EXFLOW flow cytometer (DAKEWE, Shenzhen, China).

TUNEL Staining

Cells were fixed with 4% paraformaldehyde for 30 minutes and washed with PBS 3 times. Then, the cells were incubated with 0.2% Triton X-100 for 5 minutes and stained with the In Situ Cell Apoptosis Detection Kit (Beyotime, Shanghai, China) according to the manufacturer's instructions. The cells were visualized under a fluorescence microscope (Axio

Observer D1; Zeiss, Gottingen, Germany). Positive cells were counted using Image J software.

Extracellular Acidification Rate Analysis

The XF Glycolysis Stress Test kit (Agilent, Santa Clara, CA, USA) was used for the extracellular acidification (ECAR) assay. Briefly, 1×10^4 cells were seeded into the Seahorse SF 96 cell culture microplates. Next, 10 mM glucose, 1 μm oligomycin, and 75 mM 2-DG were added to the cell medium successively at indicated time points. Seahorse SF-96 Wave software was used to analyze the results. ECAR was presented in mpH/min.

Measurement of Supernatant Lactate

The concentration of lactate in culture medium was measured by the Lactic Acid (LA) Content Assay Kit (BC2235; Solarbio, Beijing, China) according to the manufacturer's instructions. Absorbance at 570 nm was read using a microplate reader (Synergy H1, Biotek, Winooski, VT, USA), which was used to calculate the concentration of lactate.

Protein Half-Life Assay

After cycloheximide (CHX, 20 μM) was applied to the medium and at indicated time points, cells were collected, and immunoblotting was performed to evaluate the corresponding protein levels. Target bands were quantified using Image J software by normalizing to internal reference (β-actin).

Immunoprecipitation

Cells were resuspended and lysed in 0.5 mL RIPA lysis buffer (Millipore, Temecula, CA, USA) in 6-cm dishes. The samples were centrifuged to remove insoluble debris, 30 μL supernatant from each well was collected as the input, and the remaining supernatant was incubated with anti-rabbit IgG, anti-PD-L1 (sc-293425) or anti-HLA-E (sc-51621) antibodies as indicated. Immunoprecipitation was performed using Protein A/G Plus agarose Beads (Santa Cruz Technology, Santa Cruz, CA, USA), according to the manufacturer's instructions. The ubiquitination of the input and purified proteins was analyzed by Western blotting using anti-PD-L1 (ab213524), anti-HLA-E (ab300553), and anti-ubiquitin (sc-8017) antibodies.

Immunofluorescence Histochemistry

In total, 11 UM cases from the Affiliated Xuzhou Municipal Hospital of Xuzhou Medical University (Xuzhou, China) were included in this study. Informed consent was obtained from all patients. The study was approved by the Ethics Committee of the Affiliated Xuzhou Municipal Hospital of Xuzhou Medical University (Approval number: xxyll (2019) 17). Immunofluorescence staining was conducted using formalin-fixed, paraffin-embedded sections, after heat antigen retrieval following standard protocols. The following primary antibodies were used: anti-PKM (sc-365684, 1:100), anti-LDHA (sc-137243, 1:10), anti-PD-L1 (ab213524, 1:100), and anti-HLA-E (ab300553, 1:100). Secondary antibodies and dilutions used for IF staining were as follows: Alexa Fluor 488-conjugated anti-mouse IgG (H+L; #4408, CST, 1:500), and Alexa Fluor 488-conjugated anti-rabbit IgG (H+L; #4412,

CST, 1:500). To assess immunofluorescence density, five 200 × fields were selected in each slide, and the integrated density of each field was measured using ImageJ software.

Statistical Analysis

Statistical data analysis was performed using SPSS version 22.0 and GraphPad Prism 5.0. Difference analysis between the 2 groups was performed using the 2-tailed Student's t test, and difference analysis for multiple groups was performed by analysis of variance (ANOVA), followed by Tukey's post hoc test for 1-way ANOVA and Sidak post hoc test for 2-way ANOVA. Spearman's correlation test was used to analyze correlation. OS and disease-free survival (DFS) were analyzed by the Kaplan–Meier method and compared by log rank test. Cox regression was used to analyze the hazard ratio for OS and DFS. Data are reported as mean ± SD. A value of $P < 0.05$ was considered statistically significant.

RESULTS

IL-6 is a Potential Prognostic Indicator for Patients With UM and Affected the Expression of Adaptive Immunity-Associated Genes

Analysis of the Cancer Genome Atlas (TCGA) UVM dataset indicated that *IL-6* mRNA levels were increased with tumor stage in patients with UM (Fig. 1A), and although the difference was not significant, *IL-6* mRNA levels in epithelioid UM tissues were higher than those in spindle and mixed UM tissues (Fig. 1B). In addition, high *IL-6* expression was correlated with both poor OS and DFS of patients with UM (Figs. 1C, 1D); however, no significant changes were identified in the morphology of the UM cell line, C918, after continuous exposure to IL-6 (IL-6/C918; Fig. 1E). Furthermore, we performed RNA-seq to detect differences in the transcriptome profiles between the IL-6/C918 and C918 groups. In total, 5447 significantly differentially expressed transcripts ($P < 0.05$) were identified. Among these, 2745 and 2702 transcripts were up- and downregulated in IL-6/C918 cells, compared with C918 cells, respectively (Fig. 1F, Supplementary Table S2). Gene ontology (GO) functional annotation clustering of the 1472 transcripts (threshold, |log$_2$ (fold-change) | > 0.8) was conducted; the 1472 transcripts were significantly enriched in 14 terms including "innate immunity" and "immunity" ($P < 0.05$; Fig. 1G, Supplementary Table S3). As a sub-term of "immunity," the GO process "adaptive immunity" involved 14 transcripts, among which 12 were upregulated and 2 were downregulated (Fig. 1H). In summary, IL-6 expression is a marker of poor prognosis for patients with UM and IL-6 exposure may influence the expression of several immunity-associated genes in UM cells.

IL-6 Induced Immune Escape by Upregulating PD-L1 and HLA-E Levels in C918 Cells

Our transcription profiling data indicated that *PD-L1* and *HLA-E* transcript levels were significantly increased in C918 cells continuously exposed to IL-6 (IL-6/C918; Fig. 2A). Further experiments confirmed the increased mRNA and protein levels of PD-L1 and HLA-E in IL-6/C918 cells

(Figs. 2B, 2C). Consistently, upregulated levels of PD-L1 and HLA-E were detected on the membranes of IL-6/C918 cells (Fig. 2D). However, the mRNA levels of PD-L1 and HLA-E had no significant change after treatment with IL-6 in ARPE-19, a cell line derived from non-tumor cell (Supplementary Fig. S1A), suggesting that the IL-6-induced upregulation of PD-L1 and HLA-E may be specific for tumor cell, at least for C918. Relative to C918 cells, IL-6/C918 cells showed evident resistance to TALL-104 and NK-92MI cell-mediated killing (Figs. 2E, 2F). Hence, continuous exposure to IL-6 promoted PD-L1 and HLA-E expression and induced immune escape in C918 cells.

Analysis of clinical data from 40 patients with UM in TCGA database indicated that high *PD-L1* or *HLA-E* expression levels were associated with low overall OS in patients with UM (Fig. 3A). To explore the effects of PD-L1 and HLA-E on UM immune escape, we next knocked down PD-L1 and HLA-E expression in IL-6/C918 cells, and then examined the resistance of IL-6/C918 cells to killing mediated by TALL-104 and NK-92MI cells. After knockdown of PD-L1 and HLA-E in IL-6/C918 cells, the killing effect of TALL-104 and NK-92MI on IL-6/C918 cells was significantly enhanced (Figs. 3B, 3C, Supplementary Fig. S2). In summary, IL-6-induced high expression of PD-L1 and HLA-E and boosted UM cell immune escape.

IL-6 Increased Glycolysis and Production of Lactate in C918 Cells

In addition to PD-L1 and HLA-E, the KEGG pathway enrichment analysis, based on transcriptome data, revealed that continuous exposure to IL-6 induced the expression of most metabolic enzymes in the glycolysis pathway, but suppressed that of enzymes in the acetyl-CoA synthesis pathway (Fig. 4A, Supplementary Table S4). Among the three rate-limiting enzymes of the glycolysis pathway, changes in levels of transcripts encoding HK1 were negligible, while those encoding PFK (*PFKP*) and PKM were significantly increased (Supplementary Fig. S3). In addition, levels of transcripts encoding lactate dehydrogenase (LDH; *LDHA*), an enzyme key for lactate synthesis, were markedly elevated (see Supplementary Fig. S3). Moreover, PKM and LDHA mRNA and protein levels were considerably higher in IL-6/C918 cells than those in C918 cells (Figs. 4B–E). Analysis of TCGA UVM dataset suggested that *IL-6* levels were positively correlated with those of *PKM* and *LDHA* at the mRNA level (Fig. 4F). As expected, compared with C918 cells, the extracellular acidification rate and lactate release from IL-6/C918 cells were also increased (Figs. 4G, 4H). Thus, IL-6 induced lactate production by driving the glycolytic pathway in UM cells.

IL-6-Induced Lactate Increased PD-L1 and HLA-E Protein Levels and Immune Escape in C918 Cells

To explore whether IL-6-induced glycolysis plays a critical role in UM immune escape, PKM and LDHA expression were knocked down to block the glycolytic pathway and lactate production in IL-6/C918 cells, then the expression of PD-L1 and HLA-E were assessed. PD-L1 and HLA-E protein levels were decreased, but there was no significant difference in their mRNA levels after knockdown of PKM or LDHA in IL-6/C918 cells (Figs. 5A, 5B). Moreover, after inhibiting lactate production in IL-6/C918 cells using sodium oxam-
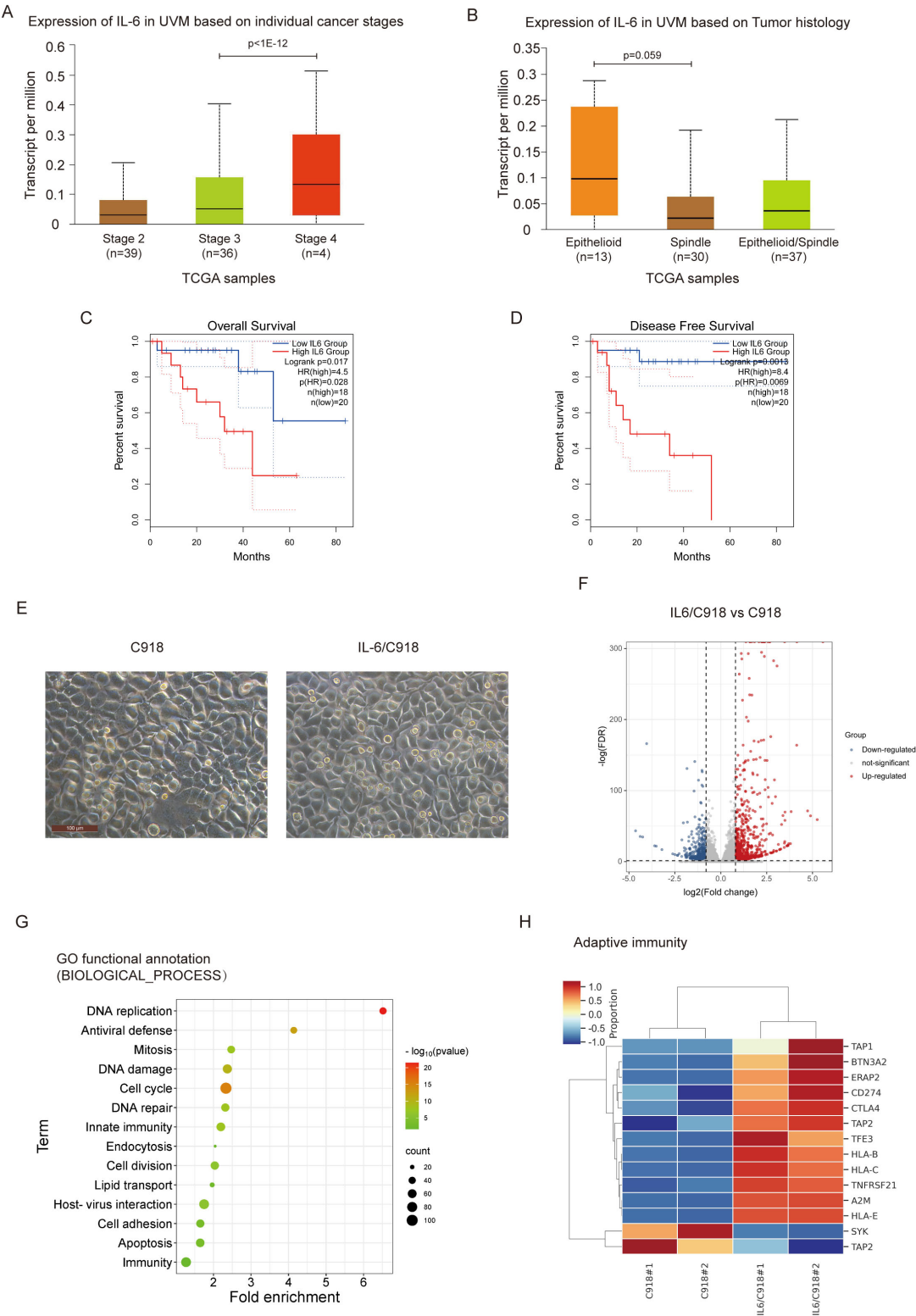
FIGURE 1.   IL-6 is a potential prognostic indicator for patients with uveal melanoma (UM) and affected the expression levels of genes associated with adaptive immunity. (A and B) Associations of cancer stage (A) and tumor histology (B) with the expression of *IL-6* in 79 and 80 UM cases, respectively, from The Cancer Genome Atlas (TCGA) database analyzed using UALCAN (http://ualcan.path.uab.edu/analysis.html). (C and D) Overall survival analysis (C) and disease-free survival analysis (D) of high and low *IL-6* expression groups in the TCGA-UVM cohort performed using GEPIA2 (http://gepia2.cancer-pku.cn/#survival). Cutoff (high = 75% and low = 25%). (E) Morphology of C918 and IL-6/C918 cells. Scale bar = 100 µm. (F) Total number of transcripts with significant changes in expression (FDR < 0.05). Of significantly differentially expressed transcripts, 883 and 589 were up- (*red dots*) and down- (*blue dots*) regulated (> 0.8-fold), respectively. (G) Gene ontology (GO) functional annotation (UP_KW_BIOLOGICAL_PROCESS) of the 1472 transcripts (threshold, |log₂ (fold-change) | > 0.8) was conducted by DAVID (https://david.ncifcrf.gov/summary.jsp). (H) Heatmap of 14 transcripts (> 0.8-fold) belonging to the gene ontology (GO) term "adaptive immunity" in IL-6/C918 versus C918; each column represents a cell sample and each row represents a gene (*Red* = increased expression and *blue* = decreased expression; *n* = 2 for each group).
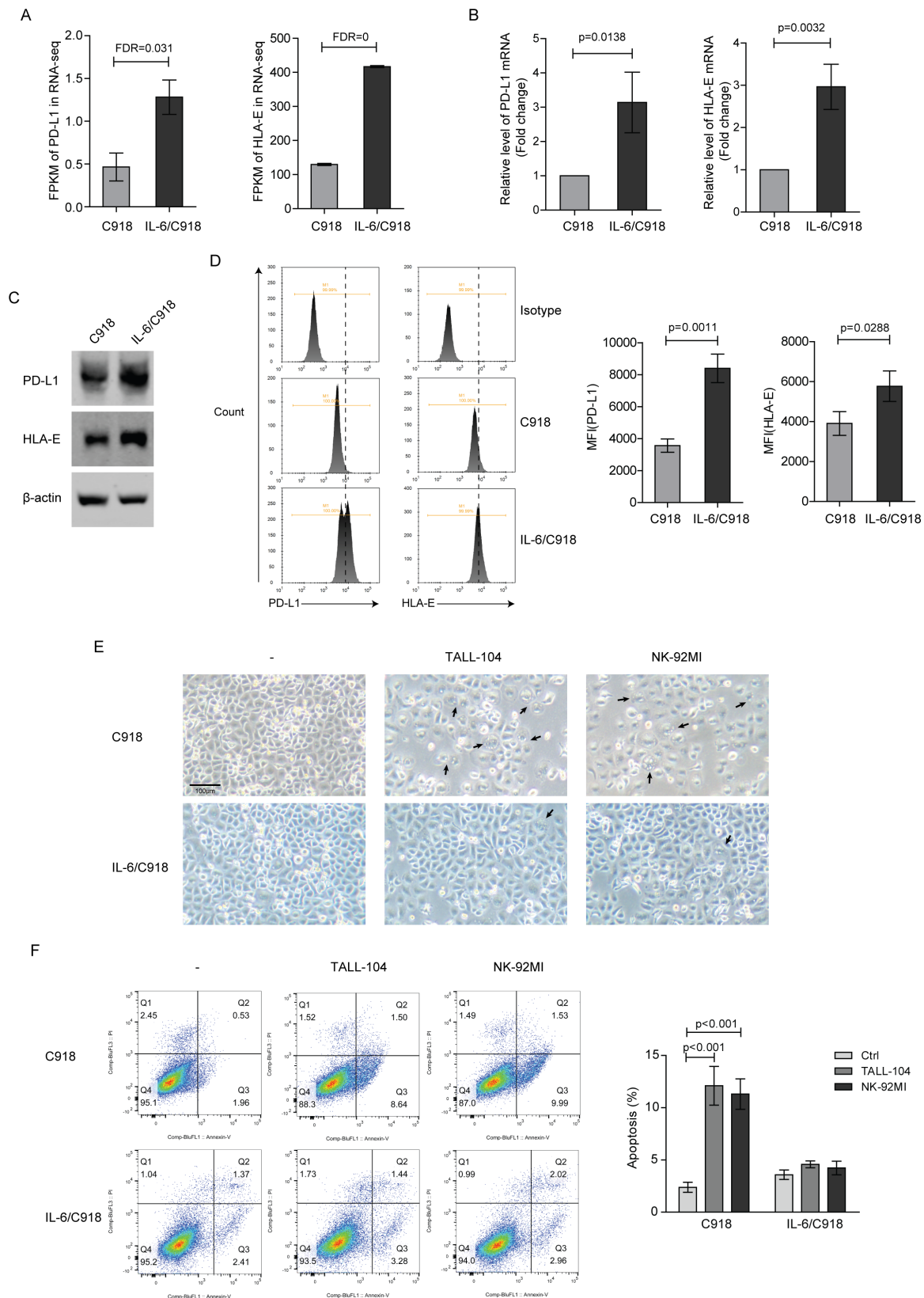
FIGURE 2. IL-6 promoted PD-L1 and HLA-E expression and induced immune escape in C918 cells. (A) The fragments per kilobase of exon model per million mapped fragments (FPKM) of *PD-L1* and *HLA-E* in IL-6/C918 and C918 cell transcriptome data. (B) Relative *PD-L1* and *HLA-E* mRNA levels in IL-6/C918 and C918 cells determined by qPCR. (C) PD-L1 and HLA-E protein levels in IL-6/C918 and C918 cells detected by Western blotting. (D) Levels of membrane PD-L1 and HLA-E in IL-6/C918 and C918 cells analyzed by flow cytometry, and mean fluorescence intensity (MFI) values of PD-L1 and HLA-E. (E) IL-6/C918 and C918 cell morphology after co-culture with TALL-104 and NK-92MI cells. *Black arrows* indicate apoptotic cells. Scale bar = 100 µm. (F) Apoptosis levels of IL-6/C918 and C918 cells after co-culture with TALL-104 and NK-92MI cells. The results of three independent experiments are presented as mean ± standard deviation.
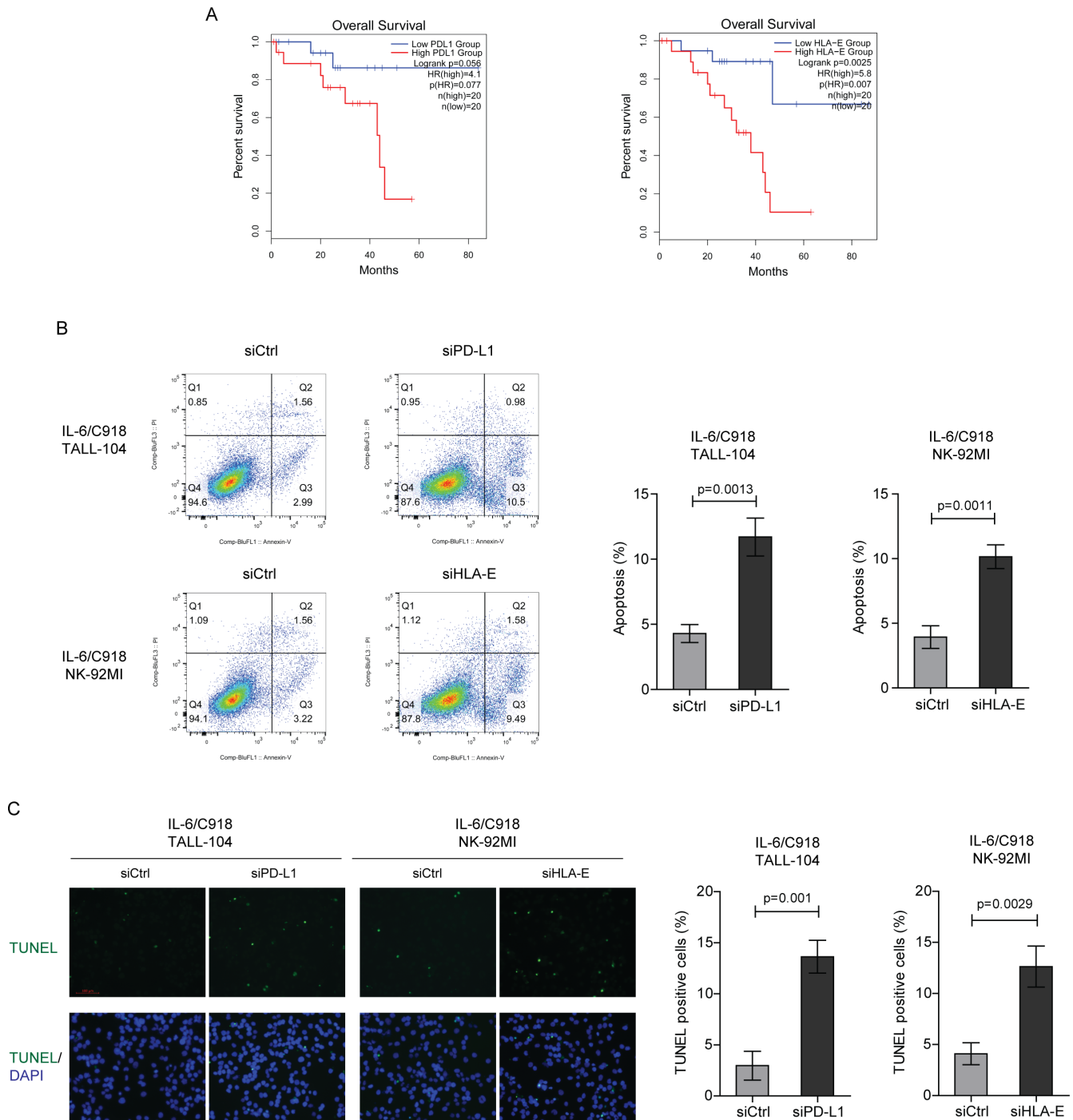
FIGURE 3. **Knockdown of PD-L1 and HLA-E increased IL-6/C918 cell immune escape.** (A) Overall survival of patients with high and low PD-L1 and HLA-E expression analyzed using GEPIA2 (http://gepia2.cancer-pku.cn/#survival) and TGCA database UM subset data; cutoff (high = 75% and low = 25%). (B) Apoptosis levels of IL-6/C918 cells with PD-L1 or HLA-E knocked down after co-culture with TALL-104 and NK-92MI cells. (C) TUNEL labeling analysis of apoptosis levels of IL-6/C918 cells with knockdown of PD-L1 or HLA-E after co-culture with TALL-104 and NK-92MI cells. Scale bar = 100 µm. The results of three independent experiments are presented as mean ± standard deviation.

ate (SO), PD-L1 and HLA-E protein levels were reduced, whereas no significant changes in their mRNA levels were detected (Figs. 5C, 5D). In C918 cells, exogenous lactate affected the protein, but not mRNA, levels of PD-L1 and HLA-E (Figs. 5E, 5F). Further, the cell-mediated killing assay

showed that inhibiting lactate with SO rendered IL-6/C918 cells more sensitive to TALL-104 and NK-92MI cell-mediated killing (Fig. 5G). Meanwhile, exogenous lactate reinforced the resistance of C918 cells to TALL-104 and NK-92MI cells (Fig. 5H).
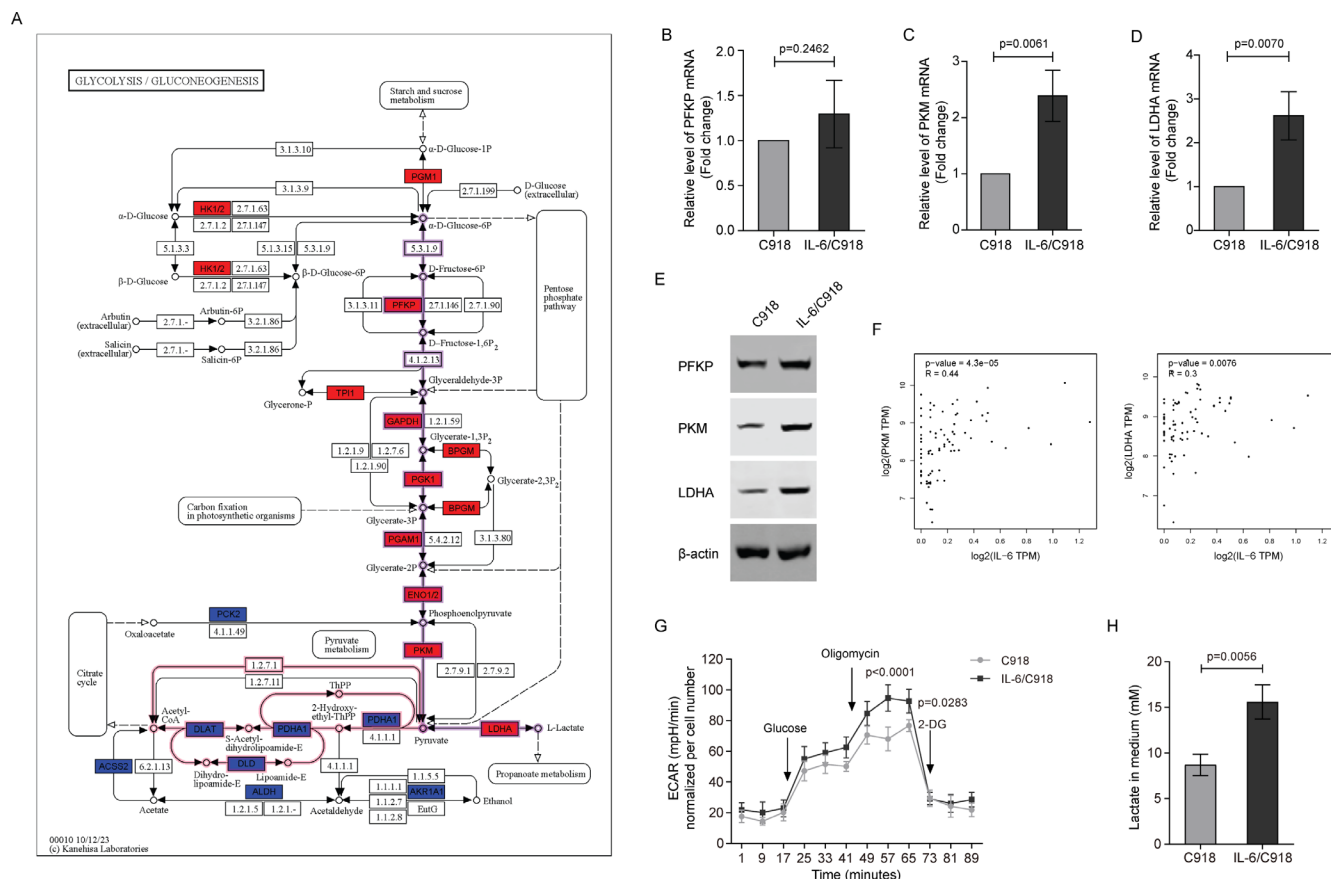
FIGURE 4. **IL-6 increased glycolysis and lactate production in C918 cells.** (A) Distribution of differentially expressed transcripts between IL-6/C918 and C918 cells identified in the glycolysis/gluconeogenesis pathway (KEGG pathway), based on transcriptome data; *red* = upregulated and *blue* = downregulated. Pathway with *blue shading* indicated the glycolysis process, and pathway with *red shading* indicated the pyruvate oxidation process. (B–D) Relative mRNA levels of *PFKP* (B), *PKM* (C), and *LDHA* (D) in IL-6/C918 and C918 cells determined by qPCR. (E) PFKP, PKM, and LDHA protein levels in IL-6/C918 and C918 cells detected by Western blotting. (F) Analysis of TCGA uveal melanoma database using GEPIA2 (http://gepia2.cancer-pku.cn/#correlation) showing correlations between *IL-6* and *PKM* or *LDHA* mRNA levels. (G) Extracellular acidification rate (ECAR) of IL-6/C918 and C918 cells. (H) Lactate concentrations in the culture medium of IL-6/C918 and C918 cells. The results of three independent experiments are presented as mean ± standard deviation.
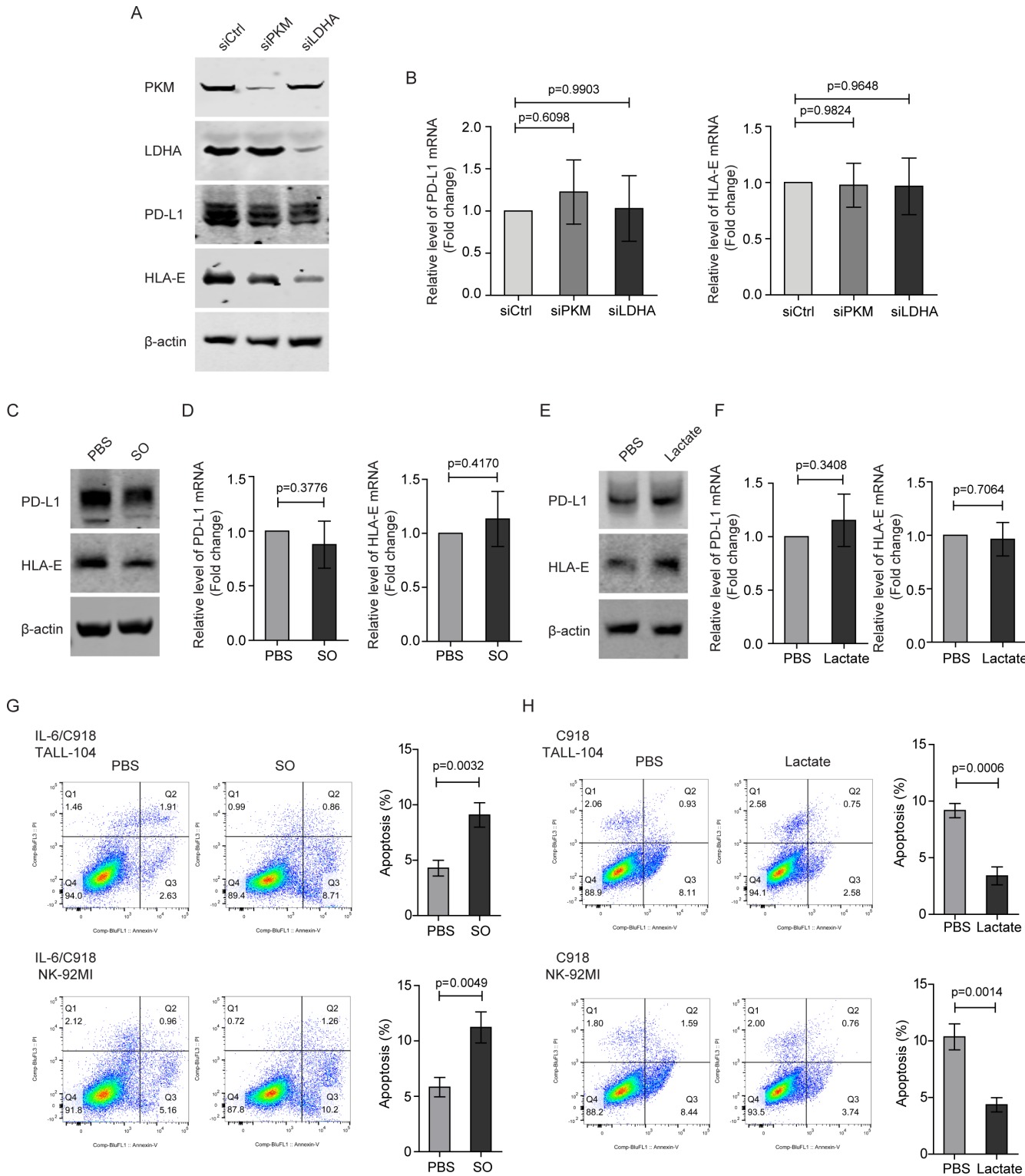
IL-6-Induced Lactate Stabilized PD-L1 and HLA-E Proteins in C918 Cells

To further explore the molecular mechanism by which IL-6 upregulated PD-L1 and HLA-E, PD-L1 and HLA-E protein stability was investigated. PD-L1 and HLA-E protein stability was higher in IL-6/C918 cells than that in C918 cells; however, the stability of these proteins was reduced in IL-6/C918 cells treated with SO (Fig. 6A). Next, to determine whether the degradation of PD-L1 and HLA-E proteins was proteasome-dependent, the proteasome inhibitor, MG-132, was applied following blockage of protein synthesis using CHX. MG-132 effectively prevented PD-L1 and HLA-E protein degradation in C918 cells treated with CHX (Fig. 6B), suggesting that IL-6 increased PD-L1 and HLA-E protein levels by inhibiting their proteasome degradation. As protein ubiquitination is often required for proteasome-dependent degradation, we next investigated PD-L1 and HLA-E protein ubiquitination. PD-L1 and HLA-E protein ubiquitination was downregulated in IL-6/C918 cells compared with C918 cells, whereas SO restored the ubiquitination of these proteins in IL-6/C918 cells (Figs. 6C, 6D). Together, our results suggest that IL-6-induced lactate produc-

tion enhances PD-L1 and HLA-E protein stability in UM cells.

IL-6-Induced Lactate Increased PD-L1 and HLA-E Protein Stability by Activating GPR81 in C918 Cells

To determine whether H^+ affects the stability of PD-L1 and HLA-E, we added $NaHCO_3$ into the culture medium to neutralize extracellular H^+; no change in PD-L1 and HLA-E expression levels was detected (Fig. 7A). Next, we investigated the G-protein-coupled lactate receptor, GPR81. As shown in Figure 7B, GPR81 knockdown reduced PD-L1 and HLA-E protein levels in IL-6/C918 cells. Given that activation of the Gi-coupled receptor, GPR81, inhibits adenylyl cyclase, which results in decreased cAMP levels, we next suppressed GPR81 downstream signaling using the cAMP analogue, bucladesine, and the adenylyl cyclase activator, forskolin. The results indicated that both bucladesine and forskolin could decrease PD-L1 and HLA-E protein levels in IL-6/C918 cells (Figs. 7C, 7D). Consistently, PD-L1 and HLA-E protein ubiquitination was induced by GPR81 knockdown
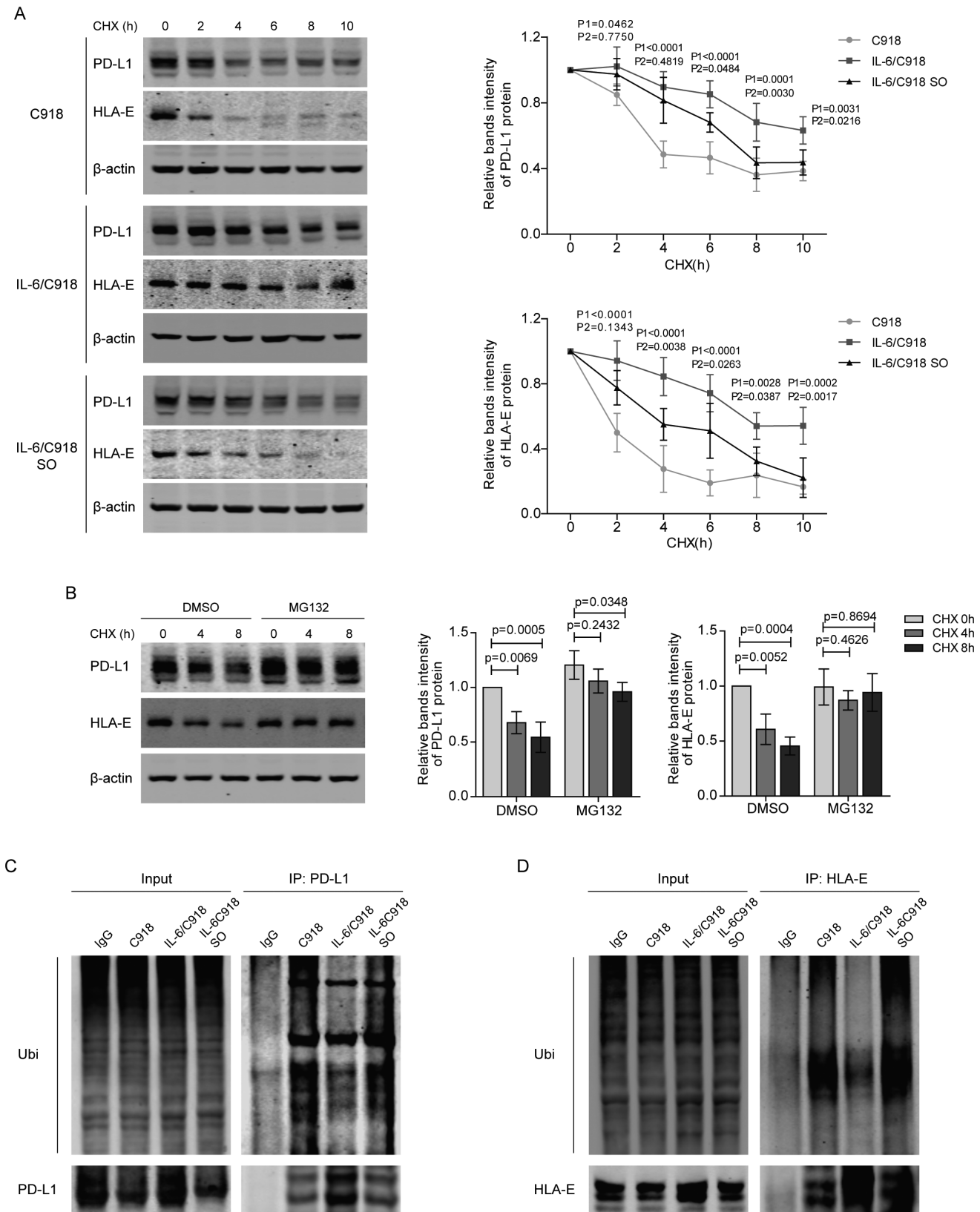
FIGURE 5. **IL-6-induced lactate increased PD-L1 and HLA-E protein levels and immune escape in C918 cells.** (A and B) PD-L1 and HLA-E protein and relative mRNA levels in IL-6/C918 cells with PKM or LDHA knocked down examined by Western blotting and qPCR. (C and D) PD-L1 and HLA-E protein and relative mRNA levels in IL-6/C918 cells treated with 50 nM sodium oxamate (SO) examined by Western blotting and qPCR. (E and F) PD-L1 and HLA-E protein and relative mRNA levels examined by Western blotting and qPCR in C918 cells treated with 20 mM lactate. (G) Apoptosis level of IL-6/C918 cells pretreated with 50 nM SO after co-culture with TALL 104 and NK-92MI cells. (H) Apoptosis level of C918 cells pretreated with 20 mM lactate after co-culture with TALL-104 and NK-92MI cells. The results of three independent experiments are presented as mean ± standard deviation.

FIGURE 6. **IL-6-induced lactate stabilized PD-L1 and HLA-E proteins in C918 cells.** (A) C918, IL-6/C918, and IL-6/C918 cells pre-treated with 50 nM sodium oxamate (SO) were exposed to 20 µM CHX for the indicated times. PD-L1 and HLA-E protein levels were detected by Western blotting. Relative band intensity was normalized to PD-L1 or HLA-E levels in cells not treated with CHX. β-actin served as an internal control. (B) C918 cells were pretreated with 10 µM MG-132 and with 20 µM CHX for the indicated times. PD-L1 and HLA-E protein levels detected by Western blotting. (C and D) Immunoprecipitation of PD-L1 or HLA-E from C918, IL-6/C918, and IL-6/C918 cells treated with 50 nM SO, and PD-L1 or HLA-E protein ubiquitination levels detected by Western blotting. The results of three independent experiments are presented as mean $\pm$ standard deviation.
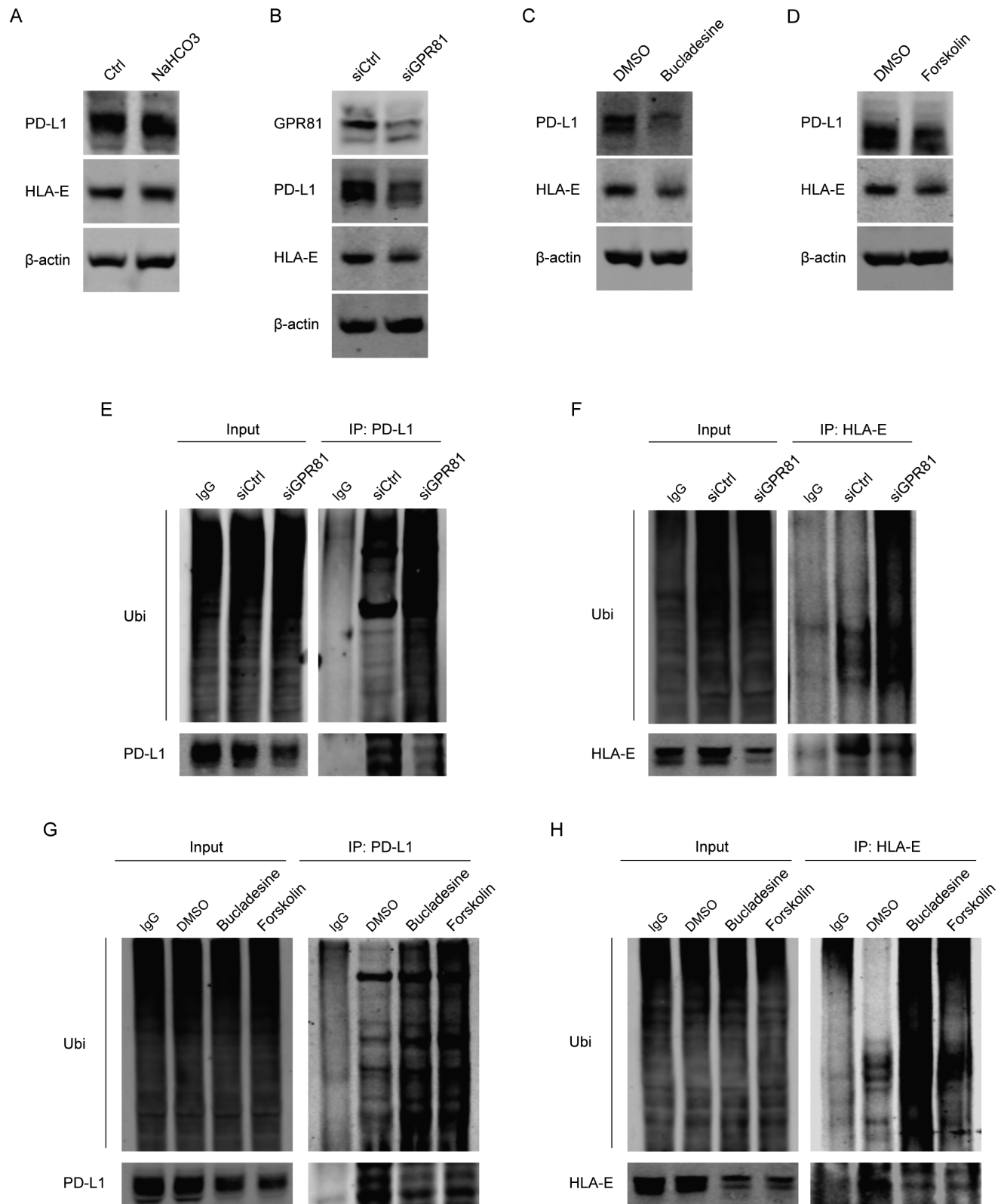
FIGURE 7. IL-6-induced lactate increased PD-L1 and HLA-E protein stability in C918 cells by activating GPR81. (A) PD-L1 and HLA-E protein levels in IL-6/C918 cells treated with 100 µM NaHCO3 detected by Western blotting. (B) PD-L1 and HLA-E protein levels detected by Western blotting in IL-6/C918 cells with GPR81 knocked down. (C and D) PD-L1 and HLA-E protein levels detected by Western blotting in IL-6/C918 cells treated with 5 µM bucladesine or 20 µM forskolin. (E and F) In IL-6/C918 cells with GPR81 knocked down, PD-L1 or HLA-E were immunoprecipitated and PD-L1 or HLA-E protein ubiquitination levels detected by Western blotting. (G and H) In IL-6/C918 cells treated with 5 µM bucladesine or 20 µM forskolin, PD-L1 or HLA-E were immunoprecipitated and PD-L1 or HLA-E protein ubiquitination levels detected by Western blotting.
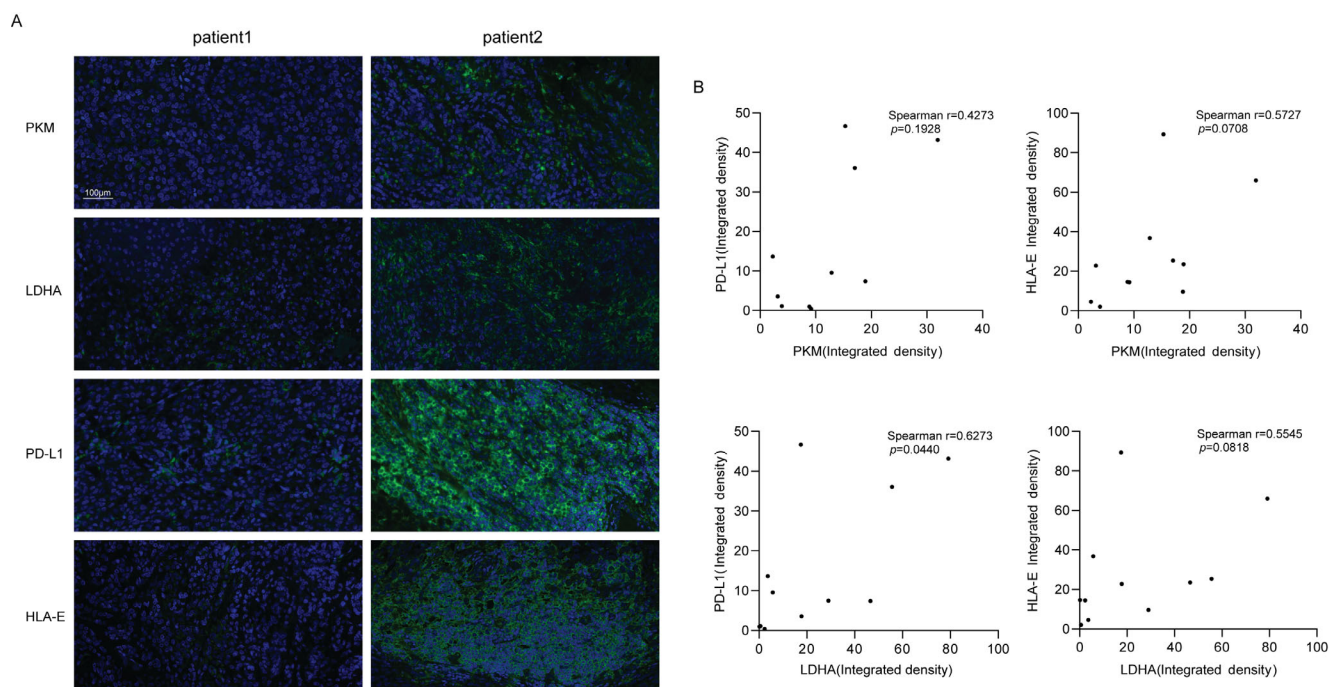
FIGURE 8. **LDHA protein levels were positively correlated with those of PD-L1 in uveal melanoma tissues.** (A) Two representative cases of low and high expression of PKM, LDHA, PD-L1, and HLA-E in clinical UM tissues. (B) The relationships of the integrated fluorescence density of PKM, LDHA, PD-L1, and HLA-E.

in IL-6/C918 cells (Figs. 7E, 7F). Bucladesine and forskolin treatment also promoted PD-L1 and HLA-E protein ubiquitination in IL-6/C918 cells (Figs. 7G, 7H). In mammalian cells, most of the effects elicited by cAMP are mediated by protein kinase A (PKA). Here, we found that the PKA inhibitor, H-89, decreased PD-L1 and HLA-E protein ubiquitination in C918 cells (Supplementary Fig. S4). In summary, activation of lactate-GPR81 signaling enhanced PD-L1 and HLA-E protein stability in UM cells.

LDHA Protein Levels Were Positively Correlated With Those of PD-L1 in UM Tissues

To verify the association between glycolysis and PD-L1/HLA-E expression, we conducted immunofluorescence histochemistry analysis to detect PKM, LDHA, PD-L1, and HLA-E protein levels in 11 UM tissues. PKM and LDHA were detected in the cytoplasm of UM cells, whereas PD-L1 and HLA-E were mainly localized in the membrane (Fig. 8A). Although further statistical analysis of integrated fluorescence density suggested a link between PKM/LDHA and PD-L1/HLA-E in UM tissues, only LDHA was significantly positively correlated with PD-L1 (Fig. 8B). Analysis of additional UM cases are needed to validate the nature of the relationships among these proteins in the context of UM.

DISCUSSION

Until recently, few studies had explored the effects of post-translational regulation, including protein glycosylation, phosphorylation, and ubiquitination, on PD-L1 expression and their impact on immune escape.[24–26] There is strong evidence that ubiquitination and de-ubiquitination of PD-L1 are critical in regulating PD-L1 protein stability,

thereby affecting PD-1/PD-L1-mediated immune escape.[26,27] Although there are no reports of HLA-E protein ubiquitination and de-ubiquitination, other MHC-I molecules can be controlled by the E3 ubiquitin-protein ligases, MARCH1 and MARCH9, which ubiquitinate cytoplasmic MHC-I for internalization into the endocytic pathway.[28,29] In the present study, we found that exogenous IL-6 not only stabilized both PD-L1 and HLA-E proteins in UM cells in a lactate-dependent manner, but also induced *PD-L1* and *HLA-E* transcription in a lactate-independent manner, although we did not explore this further. Previous studies found STAT3 as a crucial transcriptional factor of *PD-L1*, suggesting that IL-6 can induce the transcription of *PD-L1* via STAT3 signaling in UM.[30] Studies in both a murine model and a clinical trial have confirmed that a combination of antibodies blocking anti-NKG2A and anti-PD-L1 activated NK and CD8+ T cells and subsequently interfered with tumor progression.[31] Hence, understanding the mechanisms underlying IL-6-induced expression of PD-L1 and HLA-E have considerable relevance to clinical prevention of UM metastasis.

High levels of IL-6 in the TME suggest a close relationship between chronic inflammation and malignancy. IL-6 signaling (primarily through the JAK/STAT3 pathway in epithelial and immune cells) can contribute to chronic inflammation and cancer progression; for example, via influencing growth, metastasis (epithelial-mesenchymal transition [EMT]), and multidrug resistance.[32] Notably, STAT3 signaling can protect epithelial cells from the toxic effects of CD8+ T cells, promote T cell depletion, and induce PD-L1 expression on transformed epithelial cells recognized by T cells.[33] Bent et al. found that IL-6 not only inhibited chemotherapy-induced anticancer immunity but decreased the effectiveness of immune-checkpoint inhibition with anti-PD-L1 blockade.[34] In contrast, it has been reported that IL-6 can restore dendritic cell maturation

Investigative Ophthalmology & Visual Science

and is critical for macrophage function under the circumstance of tumor regression, suggesting that IL-6 is also required for antitumor immune response.[35,36] Based on the previous study that chronic IL-6 activity can activate immune-suppressive signals and attenuate the generation of a robust immune response as well as our present findings,[37] we conjecture that a consistently low level of IL-6 in TME is conducive to immune escape of tumor without causing tumor tissue destruction. Moreover, IL-6 can remodel the TME by attracting and activating related cells, such as myeloid-derived suppressor cells, tumor-associated neutrophils, regulatory T cells, and cancer stem-like cells, establishing an immunosuppressive microenvironment.[38] Therefore, IL-6 stimulation may not only affect tumor cells in UM tissue; however, we found that long-term IL-6 treatment had no significant effect on PD-L1 and HLA-E expression in the RPE cell line, ARPE-19, but did induce its EMT, suggesting that IL-6 has different biological effects on tumor and nontumor cells (see Supplementary Fig. S1). A number of clinical studies have begun to evaluate the application of anti-IL-6 drugs in cancer.[39,40] Based on our findings, we hypothesize that reducing intraocular or systemic IL-6 levels using tocilizumab may prevent UM cell immune escape, thereby inhibiting distal metastasis and improving the prognosis of patients with UM. In addition, the therapeutic effects of anti-PD-1/PD-L1 or anti-NKG2A drugs may be better for patients with UM and high IL-6 levels; however, the efficacy, method of administration (intraocular/systemic), dosage, and side effects of anti-IL-6 agents require further exploration in the context of UM.

PD-L1 is strictly regulated by the ubiquitin/proteasome system (UPS), and phosphorylation, glycosylation, and other post-translational modifications of PD-L1 protein can affect its own ubiquitination.[41] Glycogen synthetase kinase 3β (GSK3β) phosphorylates PD-L1 T180 and S184 residues, which are then recognized by several E3 ubiquitin ligases for ubiquitin-dependent degradation by the 26S proteasome.[24] S279/S283 phosphorylation by GSK3α and AMPK also promotes UPS-dependent PD-L1 degradation.[42] HLA-E ubiquitination has not been reported, although other MHC-I members are reported to be ubiquitinated and regulate immune responses to cancer cells.[43] In the present study, PKA inactivation suppressed the ubiquitination and degradation of PD-L1 and HLA-E proteins. Interestingly, we predicted that MARCHF (Membrane Associated Ring-CH-Type Finger) was a common E3 ubiquitin ligase of PD-L1 and HLA-E using UbiBrowser (data not shown). Hence, whether PKA enhances PD-L1 and HLA-E ubiquitination by directly phosphorylating these two proteins or regulating MARCHF warrants further exploration. In addition, PKA can phosphorylate 26S proteasomes, which stimulates several key proteasomal processes and degradation of ubiquitinated proteins, suggesting that PKA inhibition may also delay PD-L1 and HLA-E protein breakdown by reducing 26S proteasome activity.

Even under aerobic conditions, tumor cells tend to utilize glucose through glycolysis, a phenomenon referred to as the Warburg effect (aerobic glycolysis). A large amount of pyruvate produced during glycolysis is converted into lactate by LDH, which is released into the TME to promote tumor metastasis.[44] Melanoma cells often exhibit an enhanced Warburg effect.[45] In the present work, long exposure to IL-6 was found to induce the transcription of PKM and LDHA, two rate-limiting enzymes in the glycolysis process. Although previous reports have not revealed a clear associ-

ation between IL-6 and the Warburg effect, activation of IL-6 downstream signal transducer STAT3 promoted the Warburg effect through PKM and LDHA in tumor.[46,47] So, we speculated that STAT3 might mediate the IL-6-induced expression of PKM and LDHA in UM. Further, inhibition of glycolysis significantly weakens the invasion and metastasis phenotypes of melanoma cells.[48,49] PKM expression is negatively correlated with the survival of patients with melanoma.[50] Together, these findings suggest that an enhanced Warburg effect promotes malignant progression of melanoma. Although the Warburg effect has been widely studied in melanoma, its function in UM progression has rarely been reported. Recent studies have found a close relationship between the Warburg effect and tumor immune escape. Excess lactate produced during glycolysis leads to acidification of the TME. The decreased pH in the TME inhibits T cell proliferation and cytokine secretion, reduces the cytotoxic activity of T and NK cells, and retards dendritic cell maturation, thus providing support for tumor immune escape[51]; however, the relationship between the Warburg effect and immunosuppressive molecules expressed by tumors remains unclear. Herein, we found that the Warburg effect stabilized both PD-L1 and HLA-E proteins in UM cells. Then, we used SO to inhibit the production of lactate, the main metabolite generated by the Warburg effect, which reduced PD-L1 and HLA-E protein levels, suggesting that lactate is an essential metabolite for PD-L1 and HLA-E expression. How lactate influences PD-L1 and HLA-E expression levels is a critical question to be addressed in future investigations.

Lactic acid comprises lactate and H^+, both of which are reported to promote tumor progression.[52] To determine whether lactate, H^+, or both influence PD-L1 and HLA-E expression in UM cells, we added $NaHCO_3$ to the culture medium to clear extracellular H^+, and observed no significant change in PD-L1 and HLA-E protein levels. Furthermore, we knocked down GPR81 to study the effects of lactate, as GPR81 is the only specific lactate receptor under physiological conditions. GPR81 is widely expressed in normal and tumor tissues, and is activated by lactate, with no dependency on H^+.[52] GPR81 knockdown decreased PD-L1 and HLA-E protein stability. Previous studies have focused on the effects of lactate on immune escape, mainly including metabolic reprogramming of immune cells.[53] Nevertheless, in the autocrine pathway, tumor cell-generated lactate acts directly on GPR81 on tumor cells, influencing tumor immunosurveillance via increasing PD-L1 expression. Furthermore, Feng et al. reported that lactate-GPR81 interaction induces *PD-L1* transcription in lung cancer cells.[54] In contrast, Sasi et al. found that cAMP, a molecule decreased in response to GPR81 activity, promotes PD-L1 transcription and protein expression in diffuse large B-cell lymphoma[55]; however, we did not detect either up or downregulation of *PD-L1* mRNA levels in response to lactate or LDHA inhibitor in UM cells. GPR81 couples to the Gi-type protein subunit and mediates lactate-induced decreases in cAMP levels and PKA activity.[56] In the present study, recovering intracellular cAMP levels induced the ubiquitin-mediated degradation of PD-L1 and HLA-E proteins, and inactivation of PKA restored their stability in UM cells. These findings demonstrate that lactate-GPR81 activation upregulates PD-L1 and HLA-E levels through cAMP-PKA signaling in a non-transcription-dependent manner.

Taken together, the findings of the present study demonstrate a mechanism underlying IL-6-mediated immune escape in UM. Persistent IL-6 in the TME accelerates
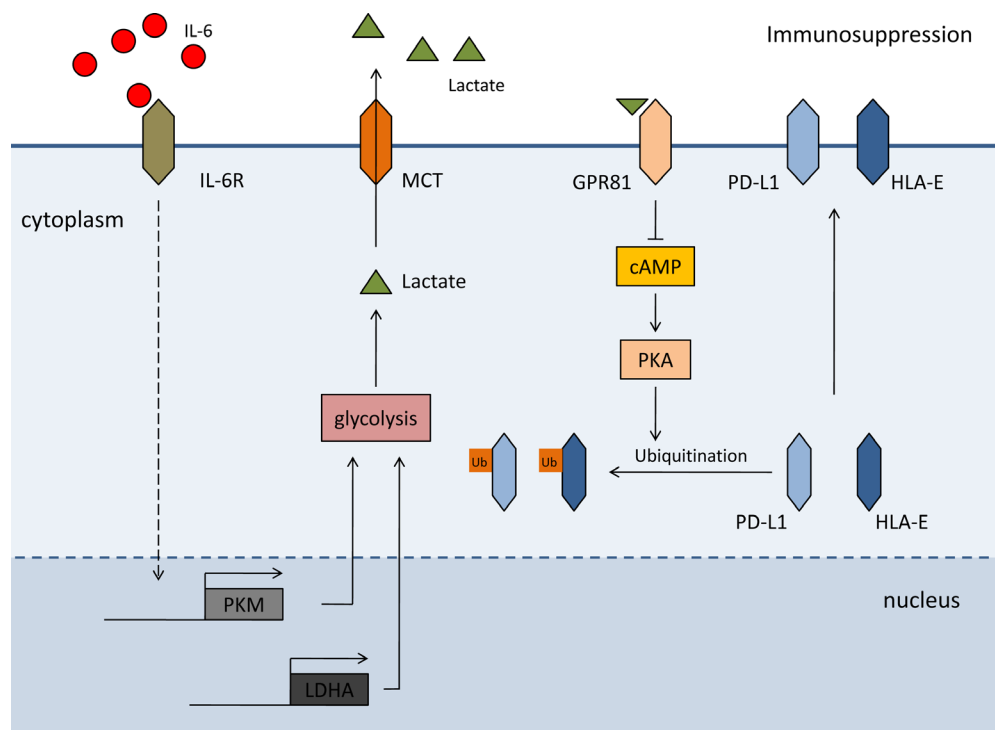
FIGURE 9. Schematic diagram showing the role of the inflammatory factor, IL-6, in enhancing the protein stability of the immunosuppressive molecules, PD-L1 and HLA-E, in uveal melanoma cells.

the glycolytic metabolic pathway by inducing PKM and LDHA expression, thereby promoting lactate production. Extracellular lactate derived from UM cells activates the lactate receptor, GPR81, to reduce intracellular cAMP levels, which in turn attenuates PKA activity, ultimately repressing the ubiquitin-dependent degradation of PD-L1 and HLA-E proteins. Finally, upregulation of PD-L1 and HLA-E protects UM from the killing effects mediated by cytotoxic T and NK cells (Fig. 9).

References

1. Jager MJ, Shields CL, Cebulla CM, et al. Uveal melanoma. *Nat Rev Dis Primers*. 2020;6(1):24.
2. Rantala ES, Hernberg MM, Piperno-Neumann S, Grossniklaus HE, Kivela TT. Metastatic uveal melanoma: the final frontier. *Prog Retin Eye Res*. 2022;90: 101041.
3. Khoja L, Atenafu EG, Suciu S, et al. Meta-analysis in metastatic uveal melanoma to determine progression free and overall survival benchmarks: an international rare cancers initiative (IRCI) ocular melanoma study. *Ann Oncol*. 2019;30(8):1370–1380.
4. Rantala ES, Kivela TT, Hernberg MM. Impact of staging on survival outcomes: a nationwide real-world cohort study of metastatic uveal melanoma. *Melanoma Res*. 2021;31(3):224–231.
5. Larkin J, Chiarion-Sileni V, Gonzalez R, et al. Five-year survival with combined nivolumab and ipilimumab in advanced melanoma. *New Engl J Med*. 2019;381(16):1535–1546.
6. Piulats JM, Espinosa E, de la Cruz Merino L, et al. Nivolumab plus ipilimumab for treatment-naive metastatic uveal melanoma: an open-label, multicenter, phase II trial by the Spanish Multidisciplinary Melanoma Group (GEM-1402). *J Clin Oncol*. 2021;39(6):586–598.
7. Pelster MS, Gruschkus SK, Bassett R, et al. Nivolumab and ipilimumab in metastatic uveal melanoma: results from a single-arm phase II study. *J Clin Oncol*. 2021;39(6):599–607.
8. Basile MS, Mazzon E, Fagone P, et al. Immunobiology of uveal melanoma: state of the art and therapeutic targets. *Front Oncol*. 2019;9:1145.
9. Sun C, Mezzadra R, Schumacher TN. Regulation and function of the PD-L1 checkpoint. *Immunity*. 2018;48(3):434–452.
10. Yang W, Chen PW, Li H, Alizadeh H, Niederkorn JY. PD-L1: PD-1 interaction contributes to the functional suppression of T-cell responses to human uveal melanoma cells in vitro. *Invest Ophthalmol Vis Sci*. 2008;49(6):2518–2525.
11. Basile MS, Mazzon E, Russo A, et al. Differential modulation and prognostic values of immune-escape genes in uveal melanoma. *PLoS One*. 2019;14(1):e0210276.
12. Kastelan S, Antunica AG, Oreskovic LB, Pelcic G, Kasun E, Hat K. Immunotherapy for uveal melanoma - current knowledge and perspectives. *Curr Med Chem*. 2020;27(8):1350–1366.

13. Olson DJ, Luke JJ. Improving therapy in metastatic uveal melanoma by understanding prior failures. *Oncoscience*. 2020;7(5-6):40–43.

14. Souri Z, Wierenga APA, Mulder A, Jochemsen AG, Jager MJ. HLA expression in uveal melanoma: an indicator of malignancy and a modifiable immunological target. *Cancers*. 2019;11(8):1132.

15. Souri Z, Wierenga APA, van Weeghel C, et al. Loss of BAP1 is associated with upregulation of the NFkB pathway and increased HLA class I expression in uveal melanoma. *Cancers*. 2019;11(8):1102.

16. Liu X, Song J, Zhang H, et al. Immune checkpoint HLA-E:CD94-NKG2A mediates evasion of circulating tumor cells from NK cell surveillance. *Cancer Cell*. 2023;41(2):272–287.e9.

17. Borst L, van der Burg SH, van Hall T. The NKG2A-HLA-E axis as a novel checkpoint in the tumor microenvironment. *Clin Cancer Res*. 2020;26(21):5549–5556.

18. Greten FR, Grivennikov SI. Inflammation and cancer: triggers, mechanisms, and consequences. *Immunity*. 2019;51(1):27–41.

19. Bronkhorst IH, Jager MJ. Inflammation in uveal melanoma. *Eye*. 2013;27(2):217–223.

20. Nagarkatti-Gude N, Bronkhorst IH, van Duinen SG, Luyten GP, Jager MJ. Cytokines and chemokines in the vitreous fluid of eyes with uveal melanoma. *Invest Ophthalmol Vis Sci*. 2012;53(11):6748–6755.

21. Babchia N, Landreville S, Clement B, Coulouarn C, Mouriaux F. The bidirectional crosstalk between metastatic uveal melanoma cells and hepatic stellate cells engenders an inflammatory microenvironment. *Exp Eye Res*. 2019;181:213–222.

22. Bao R, Surriga O, Olson DJ, et al. Transcriptional analysis of metastatic uveal melanoma survival nominates NRP1 as a therapeutic target. *Melanoma Res*. 2021;31(1):27–37.

23. Ren Y, Kumar A, Das JK, et al. Tumorous expression of NAC1 restrains antitumor immunity through the LDHA-mediated immune evasion. *J Immunother Cancer*. 2022;10(9):e004856.

24. Li CW, Lim SO, Xia W, et al. Glycosylation and stabilization of programmed death ligand-1 suppresses T-cell activity. *Nat Commun*. 2016;7:12632.

25. Chan LC, Li CW, Xia W, et al. IL-6/JAK1 pathway drives PD-L1 Y112 phosphorylation to promote cancer immune evasion. *J Clin Invest*. 2019;129(8):3324–3338.

26. Lim SO, Li CW, Xia W, et al. Deubiquitination and Stabilization of PD-L1 by CSN5. *Cancer Cell*. 2016;30(6):925–939.

27. Zhang J, Bu X, Wang H, et al. Cyclin D-CDK4 kinase destabilizes PD-L1 via cullin 3-SPOP to control cancer immune surveillance. *Nature*. 2018;553(7686):91–95.

28. Wilson KR, Liu H, Healey G, et al. MARCH1-mediated ubiquitination of MHC II impacts the MHC I antigen presentation pathway. *PLoS One*. 2018;13(7):e0200540.

29. De Angelis Rigotti F, De Gassart A, Pforr C, et al. MARCH9-mediated ubiquitination regulates MHC I export from the TGN. *Immunol Cell Biol*. 2017;95(9):753–764.

30. Xie C, Zhou X, Liang C, et al. Apatinib triggers autophagic and apoptotic cell death via VEGFR2/STAT3/PD-L1 and ROS/Nrf2/p62 signaling in lung cancer. *J Exp Clin Cancer Res*. 2021;40(1):266.

31. Herbst RS, Majem M, Barlesi F, et al. COAST: an open-label, phase II, multidrug platform study of durvalumab alone or in combination with oleclumab or monalizumab in patients with unresectable, stage III non-small-cell lung cancer. *J Clin Oncol*. 2022;40(29):3383–3393.

32. Wen Y, Zhu Y, Zhang C, et al. Chronic inflammation, cancer development and immunotherapy. *Front Pharmacol*. 2022;13:1040163.

33. Zhang Y, Velez-Delgado A, Mathew E, et al. Myeloid cells are required for PD-1/PD-L1 checkpoint activation and the establishment of an immunosuppressive environment in pancreatic cancer. *Gut*. 2017;66(1):124–136.

34. Bent EH, Millan-Barea LR, Zhuang I, Goulet DR, Frose J, Hemann MT. Microenvironmental IL-6 inhibits anti-cancer immune responses generated by cytotoxic chemotherapy. *Nat Commun*. 2021;12(1):6218.

35. Lin CS, Chen MF, Wang YS, Chuang TF, Chiang YL, Chu RM. IL-6 restores dendritic cell maturation inhibited by tumor-derived TGF-beta through interfering Smad 2/3 nuclear translocation. *Cytokine*. 2013;62(3):352–359.

36. Beyranvand Nejad E, Labrie C, van Elsas MJ, et al. IL-6 signaling in macrophages is required for immunotherapy-driven regression of tumors. *J Immunother Cancer*. 2021;9(4):e002460.

37. Hunter CA, Jones SA. IL-6 as a keystone cytokine in health and disease. *Nat Immunol*. 2015;16(5):448–457.

38. Liu Q, Yu S, Li A, Xu H, Han X, Wu K. Targeting interlukin-6 to relieve immunosuppression in tumor microenvironment. *Tumour Biol*. 2017;39(6):1010428317712445.

39. Puchalski T, Prabhakar U, Jiao Q, Berns B, Davis HM. Pharmacokinetic and pharmacodynamic modeling of an anti-interleukin-6 chimeric monoclonal antibody (siltuximab) in patients with metastatic renal cell carcinoma. *Clin Cancer Res*. 2010;16(5):1652–1661.

40. Bayliss TJ, Smith JT, Schuster M, Dragnev KH, Rigas JR. A humanized anti-IL-6 antibody (ALD518) in non-small cell lung cancer. *Expert Opin Biol Ther*. 2011;11(12):1663–1668.

41. Zhang J, Dang F, Ren J, Wei W. Biochemical aspects of PD-L1 regulation in cancer immunotherapy. *Trends Biochem Sci*. 2018;43(12):1014–1032.

42. Wu Y, Zhang C, Liu X, et al. ARIH1 signaling promotes anti-tumor immunity by targeting PD-L1 for proteasomal degradation. *Nat Commun*. 2021;12(1):2346.

43. Cano F, Lehner PJ. A novel post-transcriptional role for ubiquitin in the differential regulation of MHC class I allotypes. *Mol Immunol*. 2013;55(2):135–138.

44. Lu J. The Warburg metabolism fuels tumor metastasis. *Cancer Metastasis Rev*. 2019;38(1-2):157–164.

45. Scott DA, Richardson AD, Filipp FV, et al. Comparative metabolic flux profiling of melanoma cell lines: beyond the Warburg effect. *J Biol Chem*. 2011;286(49):42626–42634.

46. Bi YH, Han WQ, Li RF, et al. Signal transducer and activator of transcription 3 promotes the Warburg effect possibly by inducing pyruvate kinase M2 phosphorylation in liver precancerous lesions. *World J Gastroenterol*. 2019;25(16):1936–1949.

47. Huo N, Cong R, Sun ZJ, et al. STAT3/LINC00671 axis regulates papillary thyroid tumor growth and metastasis via LDHA-mediated glycolysis. *Cell Death Dis*. 2021;12(9):799.

48. Bettum IJ, Gorad SS, Barkovskaya A, et al. Metabolic reprogramming supports the invasive phenotype in malignant melanoma. *Cancer Lett*. 2015;366(1):71–83.

49. Yang X, Zhao H, Yang J, et al. MiR-150-5p regulates melanoma proliferation, invasion and metastasis via SIX1-mediated Warburg effect. *Biochem Biophys Res Commun*. 2019;515(1):85–91.

50. Welinder C, Pawlowski K, Szasz AM, et al. Correlation of histopathologic characteristics to protein expression and function in malignant melanoma. *PLoS One*. 2017;12(4):e0176167.

51. Ganapathy-Kanniappan S. Linking tumor glycolysis and immune evasion in cancer: emerging concepts and therapeutic opportunities. *Biochim Biophys Acta Rev Cancer*. 2017;1868(1):212–220.

52. Brown TP, Ganapathy V. Lactate/GPR81 signaling and proton motive force in cancer: Role in angiogenesis, immune escape, nutrition, and Warburg phenomenon. *Pharmacol Ther*. 2020;206:107451.

53. Luo Y, Li L, Chen X, Gou H, Yan K, Xu Y. Effects of lactate in immunosuppression and inflammation: progress and prospects. *Int Rev Immunol*. 2022;41(1):19–29.

54. Feng J, Yang H, Zhang Y, et al. Tumor cell-derived lactate induces TAZ-dependent upregulation of PD-L1 through GPR81 in human lung cancer cells. *Oncogene*. 2017;36(42):5829–5839.

55. Sasi B, Ethiraj P, Myers J, et al. Regulation of PD-L1 expression is a novel facet of cyclic-AMP-mediated immunosuppression. *Leukemia*. 2021;35(7):1990–2001.

56. Sun S, Li H, Chen J, Qian Q. Lactic acid: no longer an inert and end-product of glycolysis. *Physiology*. 2017;32(6):453–463.